Nonlinear Adaptive Burn Control of Two-Temperature Tokamak Plasmas

Vincent Graber and Eugenio Schuster

Abstract— **Generating electricity by harnessing the energy released from nuclear fusion reactions is an emerging environmentally-friendly approach. A tokamak is a toroidal device where a hot ionized gas, or plasma, is magnetically confined at temperatures suitable for nuclear fusion. Future commercial tokamaks will require proper control of external actuators, such as particle injection and auxiliary heating, to regulate the density and temperature of burning (fusion producing) plasmas. This is known as burn control, and it is one of the greatest challenges in fusion reactors. Engineering limitations may force upcoming reactors, such as ITER, to operate at conditions where the thermonuclear reaction rate increases as the plasma temperature increases. Plasma operation necessitates active control schemes to precisely regulate the nonlinear burning plasma dynamics. Controllers based on linearized models may fail under large perturbations. Therefore, control designs that consider the nonlinearities of the multivariable plasma dynamics are indeed necessary. In this work, a control algorithm is proposed based on a nonlinear, volume-averaged, two-temperature model. This zero-dimensional (0D) model consists of particle and energy conservation equations. Since plasmas are highly complex systems, any reduced control-oriented model is bound to contain uncertainty. The considered model contains uncertainties in the relationship between the ion and electron temperatures, the plasma confinement scalings, and the particle recycling that results from plasma-wall interactions. Adaptive control laws are employed to stabilize the system despite these numerous uncertainties. A simulation study illustrates the effectiveness of the presented adaptive controller.**

I. INTRODUCTION

The attractiveness of fusion energy is due to its almost limitless fuel supply, zero greenhouse gas emission, impossibility of a catastrophic meltdown, and short-lived nuclear waste. The first generation of fusion reactors are slated to be powered by the fusion of deuterium and tritium ions (hydrogen isotopes). In a deuterium-tritium (DT) reaction, the hydrogenic ions combine into a tightly-bound alpha-particle (helium) and give birth to an energetic neutron. Since the products have less mass than the reactants, the reaction is exothermic. For fusion to occur, the positively charged DT particles must overcome their Coulomb repulsion. This is achieved by heating the DT gas to $\sim$100 million degrees, becoming fully ionized (plasma). Tokamaks [1] confine extremely hot plasmas by forcing ions and electrons to move along magnetic field lines that wrap around the torus-shaped device. The neutral neutrons escape the magnetic confinement, and their kinetic energy is used to generate electricity. A central goal of nuclear fusion research is to produce a burning plasma that mostly heats itself with the energy released from the nuclear fusion reactions.

The crucial next step in the development of magnetic fusion technology is ITER, which will be the first tokamak to sustain a burning plasma, and it will demonstrate the viability and safety of fusion energy production. In ITER, a fusion to auxiliary power ratio, Q, of 10 is sought. To maintain this burn condition, active control of plasma temperature and density is required. In addition to auxiliary heating, ITER will have two hydrogen pellet injectors for deep core fueling and an impurity pellet injector [2]. If necessary, impurity injection can be used to decrease the plasma energy by increasing the radiation losses. Previous work [3], [4], [5] has made use of these actuators to develop burn controllers with different levels of sophistication.

During operation, hydrogen and impurity particles will be recycled and sputtered from the reactor walls, divertor and other material surfaces. Recycling describes the various processes that may occur when an ion exits the plasma and strikes some plasma facing component [6]. The incident ion either immediately reflects back into the plasma or implants itself into the material. After implantation, the particle might get trapped in the material. Alternatively, the particle could randomly diffuse out of the material, re-emit into the plasma and contribute to the recycling flux. As considered in this work and previous work [7], [8], modeling of recycling conditions and plasma confinement properties unavoidably contains a certain level of uncertainty.

The energetic alpha-particle produced in the DT reaction deposits its kinetic energy into the surrounding plasma. Most of the energy will heat the electrons, and the rest will heat the ions. As a result, the electrons and ions will have different temperatures. Auxiliary power sources such as ion cyclotron range of frequencies (ICRF) heating and electron cyclotron resonant heating (ECRH) can further differentiate the ion and electron temperatures. However, most of the previous work on model-based burn control makes the simplifying assumption that the ion and electron temperatures are the same. In contrast, the controller proposed in this work is developed using a two-temperature model. Furthermore, uncertainty in the relationship between the ion and electron energies is taken into account.

In this work, a nonlinear control-design approach is followed based on a two-temperature model to synthesize an algorithm that modulates the external heating and fueling rates to drive the plasma to desired states. Using Lyapunov analysis [9], we construct adaptive laws that stabilize the system's equilibrium despite the aforementioned uncertainties.

This work was supported in part by the U.S. Department of Energy (DE-SC0010661). V. Graber (graber@lehigh.edu) and E. Schuster are with the Department of Mechanical Engineering and Mechanics, Lehigh University, Bethlehem, PA 18015, USA.

This paper is organized as follows. The two-temperature plasma model is described in Section II. The control objectives are stated in Section III. In Section IV, the stabilizing adaptive control laws are formulated. A simulation study is presented in Section V. Finally, in Section VI, conclusions are drawn and possible future work is presented.

II. BURNING PLASMA MODEL

The zero-dimensional, volume-averaged model considers four different ions – deuterium, tritium, alpha-particles and impurity particles characterized by an average atomic number. The electrons and ions are considered to have different energies and temperatures. The energy ratio is defined as

$$\rho \triangleq \frac{E_e}{E_i}, \tag{1}$$

where E_e and E_i are the electron and ion energies, respectively. The total plasma energy is defined as

$$E = E_i + E_e = \frac{3}{2}(n_D + n_T + n_\alpha + n_I)T_i + \frac{3}{2}n_e T_e, \tag{2}$$

where T_i and T_e are the ion and electron temperatures, respectively, and n_D, n_T, n_α, and n_I are the deuterium, tritium, alpha-particle and impurity densities, respectively. The electron density is given by the quasi-neutrality condition

$$n_e = n_D + n_T + 2n_\alpha + Z_I n_I, \tag{3}$$

where Z_I is the impurity atomic number. Note that $n_D + n_T + n_\alpha + n_I$ in (2) represents the total ion density. The total plasma density is simply

$$n = n_D + n_T + n_\alpha + n_I + n_e. \tag{4}$$

The equation governing the total energy balance is

$$\frac{dE}{dt} = -\frac{E}{\tau_E} + P_\alpha - P_{rad} + P_{Ohm} + P_{aux}, \tag{5}$$

where P_α is the alpha-particle heating from the fusion reactions, P_{rad} is the bremsstrahlung radiation losses, P_{Ohm} is the ohmic heating and P_{aux} is the controlled auxiliary power. The term $-E/\tau_E$ represents the transport of energy out of the plasma, and τ_E is the energy confinement time. Each fusion reaction births an alpha-particle, which deposits 3.52 MeV (Q_α) of energy into the plasma. The alpha-particle power is $P_\alpha = Q_\alpha S_\alpha$ where $S_\alpha = n_D n_T \langle\sigma\nu\rangle$ is the source of alpha-particles. The DT reactivity is given by the expression (a_i and r are found in [10])

$$\langle\sigma\nu\rangle = exp\Big(a_1 T_i^{-r} + a_2 + a_3 T_i + a_4 T_i^2 + a_5 T_i^3 + a_6 T_i^4\Big). \tag{6}$$

While the DT reactivity depends on the temperature of the ions, the radiation loss and ohmic heating powers are dependent on the electron temperature and are expressed as

$$P_{rad} = 5.5 \times 10^{-37} Z_{eff} n_e^2 \sqrt{T_e}, \tag{7}$$

$$P_{Ohm} = 2.8 \times 10^{-9} Z_{eff} I_p^2 a^{-4} T_e^{-3/2}, \tag{8}$$

where $Z_{eff} = (n_D + n_T + 4n_\alpha + Z_I^2 n_I)/n_e$ is the effective atomic number, I_p is the plasma current, a is the minor radius of the plasma, and T_e is expected in keV [11].

For the purposes of control design, we write the energy balance equation (5) in terms of E_i and ρ. Recalling (1), (2), (7) and (8), the ion energy balance equation is given by

$$\frac{dE_i}{dt} = -\frac{E_i}{\tau_E} + \frac{1}{1+\rho}Q_\alpha S_\alpha - \frac{\rho^{1/2}}{1+\rho}P_{rad}^\star + \frac{\rho^{-3/2}}{1+\rho}P_{Ohm}^\star + \frac{1}{1+\rho}P_{aux}, \tag{9}$$

$$P_{rad}^\star = 5.5 \times 10^{-37} Z_{eff} n_e^2 \sqrt{\frac{2}{3}\frac{E_i}{n_e}}, \tag{10}$$

$$P_{Ohm}^\star = 2.8 \times 10^{-9} Z_{eff} I_p^2 a^{-4} \left(\frac{2}{3}\frac{E_i}{n_e}\right)^{-3/2}. \tag{11}$$

We use the IPB98(y,2) scaling law [12] for τ_E. It is

$$\tau_E = H_H \tau_E^{sc} \triangleq H_H K P^{-0.69} V^{-0.69} n_{e_{19}}^{0.41}, \tag{12}$$

where $K = 0.0562 I_p^{0.93} B_T^{0.15} M^{0.19} R^{1.97} \epsilon^{0.58} \kappa^{0.78}$, H_H is the H-factor, which depends on the quality of the plasma confinement, $P = P_\alpha + P_{aux} - P_{rad} + P_{Ohm}$ is the total plasma power in MWm^{-3}, V is the plasma volume, n_e is the electron density in 10^{19} m^{-3}, B_T is the toroidal field, $M = 3\gamma + 2(1-\gamma)$ is the effective mass, R is the plasma major radius, $\epsilon = a/R$ is the aspect ratio, and κ is the vertical elongation at the 95% flux surface. The ITER values for I_p, B_T, R, a, κ and V are 15 MA, 5.3 T, 6.2 m, 2 m, 1.7 and 837 m^3, respectively. The tritium fraction, γ, is defined as

$$\gamma \triangleq \frac{n_T}{n_H}, \tag{13}$$

where $n_H = n_D + n_T$ is the total hydrogen density.

The particle density balance equations are

$$\begin{aligned}
\frac{dn_\alpha}{dt} &= -\frac{n_\alpha}{\tau_\alpha} + S_\alpha, \\
\frac{dn_D}{dt} &= -\frac{n_D}{\tau_D} + f_{eff} S_D^R - S_\alpha + S_D, \\
\frac{dn_T}{dt} &= -\frac{n_T}{\tau_T} + f_{eff} S_T^R - S_\alpha + S_T, \\
\frac{dn_I}{dt} &= -\frac{n_I}{\tau_I} + S_I + S_I^{sp},
\end{aligned} \tag{14}$$

where S_D^R, S_T^R and S_I^{sp} are particle fluxes resulting from plasma-wall interactions, while S_D, S_T and S_I are the controlled injection rates of deuterium, tritium and impurities, respectively. Ion confinement times are scaled with τ_E such that $\tau_\alpha = k_\alpha \tau_E$, $\tau_D = k_D \tau_E$, $\tau_T = k_T \tau_E$ and $\tau_I = k_I \tau_E$. The recycling sources of the fuel ions are modeled as

$$S_D^R = \frac{1}{1 - f_{ref}(1 - f_{eff})} \Bigg\{ f_{ref} \frac{n_D}{\tau_D} + \left(\frac{n_D}{\tau_D} + \frac{n_T}{\tau_T}\right) (1 - \gamma^{PFC}) \left[\frac{(1 - f_{ref}(1 - f_{eff}))R^{eff}}{1 - R^{eff}(1 - f_{eff})} - f_{ref} \right] \Bigg\}, \tag{15}$$

$$S_T^R = \frac{1}{1 - f_{ref}(1 - f_{eff})} \Bigg\{ f_{ref} \frac{n_T}{\tau_T} + \left(\frac{n_D}{\tau_D} + \frac{n_T}{\tau_T}\right) \gamma^{PFC} \left[\frac{(1 - f_{ref}(1 - f_{eff}))R^{eff}}{1 - R^{eff}(1 - f_{eff})} - f_{ref} \right] \Bigg\}, \tag{16}$$

where f_{eff} is the recycled particle fueling efficiency, f_{ref} is the fraction of particles reflected back into the plasma, γ^{PFC} is the tritium fraction of the re-emitted particles, and R^{eff} is the global recycling coefficient [6]. The sputtering source of impurities depends on the total plasma density, i.e. $S_I^{sp} = f_I^{sp}(n/\tau_I + \dot{n})$, where f_I^{sp} is the sputtering fraction.

III. CONTROL APPROACH AND OBJECTIVES

In this work, we consider the energy ratio (ρ), H-factor (H_H), confinement constants (k_α, k_D, k_T, k_I) and recycling parameters (f_{eff}, f_{ref}, R^{eff}, γ^{PFC}, f_I^{sp}) to be uncertain constants. From a control-design perspective, the ion energy E_i is considered to be one of the model states, while E and E_e are related to E_i through the uncertain parameter ρ.

To ease the design process, (9) and (14) are written as

$$\begin{aligned}
\frac{dn_\alpha}{dt} &= -\theta_5^\star \frac{n_\alpha}{\tau_E^{sc}} + S_\alpha,\\
\frac{dn_D}{dt} &= -\theta_6^\star \frac{n_D}{\tau_E^{sc}} + \theta_9^\star \frac{n_T}{\tau_E^{sc}} - S_\alpha + S_D,\\
\frac{dn_T}{dt} &= -\theta_7^\star \frac{n_T}{\tau_E^{sc}} + \theta_{10}^\star \frac{n_D}{\tau_E^{sc}} - S_\alpha + S_T,\\
\frac{dE_i}{dt} &= -\theta_4^\star \frac{E_i}{\tau_E^{sc}} + \theta_1^\star P_\alpha - \theta_2^\star P_{rad}^\star + \theta_3^\star P_{Ohm}^\star + \theta_1^\star P_{aux},\\
\frac{dn_I}{dt} &= -\theta_8^\star \frac{n_I}{\tau_E^{sc}} + S_I + \theta_{11}^\star \frac{n}{\tau_E^{sc}} + \theta_{12}^\star \dot{n},
\end{aligned} \tag{17}$$

where $\theta_i^\star$ for $i \in \{1, ..., 12\}$ are the nominal lumped uncertainty parameters (for brevity, their formulas are not presented here but can be easily inferred from (9) and (14)). The desired equilibrium values ($\bar{n}_\alpha$, $\bar{n}_D$, $\bar{n}_T$, $\bar{E}_i$, $\bar{n}_I$, $\bar{P}_{aux}$, $\bar{S}_D$, $\bar{S}_T$, $\bar{S}_I \equiv 0$) are determined by setting the time derivatives in (17) to zero and solving the closed system for three predetermined quantities (i.e. E_i, n, γ).

The deviations of the states from their desired equilibrium can be defined as $\tilde{n}_\alpha = n_\alpha - \bar{n}_\alpha$, $\tilde{n}_D = n_D - \bar{n}_D$, $\tilde{n}_T = n_T - \bar{n}_T$, $\tilde{E}_i = E_i - \bar{E}_i$ and $\tilde{n}_I = n_I - \bar{n}_I$. Then the system model can be rewritten as

$$\begin{aligned}
\dot{\tilde{n}}_\alpha =& -\theta_5^\star \frac{\bar{n}_\alpha}{\tau_E^{sc}} - \theta_5^\star \frac{\tilde{n}_\alpha}{\tau_E^{sc}} + S_\alpha,\\
\dot{\tilde{n}}_D =& -\theta_6^\star \frac{\bar{n}_D}{\tau_E^{sc}} - \theta_6^\star \frac{\tilde{n}_D}{\tau_E^{sc}} + \theta_9^\star \frac{\bar{n}_T}{\tau_E^{sc}} + \theta_9^\star \frac{\tilde{n}_T}{\tau_E^{sc}} - S_\alpha + S_D,\\
\dot{\tilde{n}}_T =& -\theta_7^\star \frac{\bar{n}_T}{\tau_E^{sc}} - \theta_7^\star \frac{\tilde{n}_T}{\tau_E^{sc}} + \theta_{10}^\star \frac{\bar{n}_D}{\tau_E^{sc}} + \theta_{10}^\star \frac{\tilde{n}_D}{\tau_E^{sc}} - S_\alpha + S_T,\\
\dot{\tilde{E}}_i =& -\theta_4^\star \frac{\bar{E}_i}{\tau_E^{sc}} - \theta_4^\star \frac{\tilde{E}_i}{\tau_E^{sc}} + \theta_1^\star P_\alpha - \theta_2^\star P_{rad}^\star\\
&+ \theta_3^\star P_{Ohm}^\star + \theta_1^\star P_{aux},\\
\dot{\tilde{n}}_I =& -\theta_8^\star \frac{\bar{n}_I}{\tau_E^{sc}} - \theta_8^\star \frac{\tilde{n}_I}{\tau_E^{sc}} + S_I + \theta_{11}^\star \frac{\bar{n}}{\tau_E^{sc}} + \theta_{11}^\star \frac{\tilde{n}}{\tau_E^{sc}} + \theta_{12}^\star \dot{\tilde{n}}.
\end{aligned} \tag{18}$$

Our control objective is to drive (18) to its equilibrium at the origin despite model uncertainties. Adaptive control laws are used to stabilize the equilibria of the $\tilde{E}_i$, $\tilde{n}$ and $\tilde{\gamma}$ subsystems.

IV. ADAPTIVE CONTROL ALGORITHM

Energy Control: To begin the control design, we seek to drive $\tilde{E}_i$ to zero by reducing the energy equation in (18) to $\dot{\tilde{E}}_i = -\theta_4^\star \tilde{E}_i / \tau_E^{sc}$ by satisfying

$$\theta_4^\star \frac{\bar{E}_i}{\tau_E^{sc}} = \theta_1^\star P_\alpha - \theta_2^\star P_{rad}^\star + \theta_3^\star P_{Ohm}^\star + \theta_1^\star P_{aux}. \tag{19}$$

Since $\tau_E^{sc} > 0$ and $\theta_4^\star > 0$, the equilibrium of $\tilde{E}_i$ subsystem is exponentially stable. Condition (19) can be met in several ways. Here, we consider two approaches. The auxiliary power, P_{aux}, can directly regulate $\tilde{E}_i$. If P_{aux} is driven to zero during large positive perturbations, impurity injection, S_I, is relied upon. Input S_I can increase the impurity content and subsequently the radiation losses, P_{rad}, to satisfy (19).

To determine the auxiliary heating control law, we take the Lyapunov function

$$V_E = \frac{k_1^2 \tilde{E}_i^2}{2} + \tilde{\theta}_E^T \frac{\Gamma^{-1}}{2} \tilde{\theta}_E, \tag{20}$$

where $\tilde{\theta}_E = [\tilde{\theta}_1 \quad \tilde{\theta}_2 \quad \tilde{\theta}_3 \quad \tilde{\theta}_4]^T$ defines the vector of the estimate errors of the lumped parameters, Γ is a positive definite matrix, and k_1 is a positive constant. The controller's current estimate of these lumped parameters, $\hat{\theta}_E$, is given by $\hat{\theta}_E = \tilde{\theta}_E + \theta_E^\star$. Taking the time derivative of (20) yields

$$\dot{V}_E = k_1^2 \tilde{E}_i \dot{\tilde{E}}_i + \tilde{\theta}_E^T \Gamma^{-1} \dot{\tilde{\theta}}_E, \tag{21}$$

where $\dot{\tilde{\theta}}_E = \dot{\hat{\theta}}_E$ since $\theta_E^\star$ is constant. Substituting $\dot{\tilde{E}}_i$ from (18), gives

$$\begin{aligned}
\dot{V}_E =& k_1^2 \tilde{E}_i \Big[-\theta_4^\star \frac{\tilde{E}_i}{\tau_E^{sc}} - \theta_4^\star \frac{\bar{E}_i}{\tau_E^{sc}} + \theta_1^\star P_\alpha - \theta_2^\star P_{rad}^\star\\
&+ \theta_3^\star P_{Ohm}^\star + \hat{\theta}_1 P_{aux} - \tilde{\theta}_1 P_{aux} \Big] + \tilde{\theta}_E^T \Gamma^{-1} \dot{\tilde{\theta}}_E.
\end{aligned} \tag{22}$$

Motivated by the certainty equivalence principle [13],

$$P_{aux} = \frac{1}{\hat{\theta}_1} \Big[\hat{\theta}_4 \frac{\bar{E}_i}{\tau_E^{sc}} - \hat{\theta}_1 P_\alpha + \hat{\theta}_2 P_{rad}^\star - \hat{\theta}_3 P_{Ohm}^\star \Big], \tag{23}$$

is taken as a control law to transform (22) to

$$\begin{aligned}
\dot{V}_E =& -\frac{k_1^2 \tilde{E}_i^{\,2}}{\tau_E^{sc}} \theta_4^\star + \tilde{\theta}_E^T \Gamma^{-1} \dot{\tilde{\theta}}_E - k_1^2 \tilde{E}_i (P_\alpha + P_{aux}) \tilde{\theta}_1\\
&+ k_1^2 \tilde{E}_i P_{rad}^\star \tilde{\theta}_2 - k_1^2 \tilde{E}_i P_{Ohm}^\star \tilde{\theta}_3 + k_1^2 \tilde{E}_i \frac{\bar{E}_i}{\tau_E^{sc}} \tilde{\theta}_4.
\end{aligned} \tag{24}$$

If the nominal parameters are known ($\hat{\theta}_E = \theta_E^\star \Leftrightarrow \tilde{\theta}_E \equiv 0$),

$$\dot{V}_E = -\frac{k_1^2 \tilde{E}_i^{\,2}}{\tau_E^{sc}} \theta_4^\star \leq 0. \tag{25}$$

The nominal values of the lumped parameters are not always known ($\hat{\theta}_E \neq \theta_E^\star$), so we take the adaptive law

$$\dot{\hat{\theta}}_E = \dot{\tilde{\theta}}_E = \Gamma \begin{bmatrix} (P_\alpha + P_{aux}) k_1^2 \tilde{E}_i \\ -P_{rad}^\star k_1^2 \tilde{E}_i \\ P_{Ohm}^\star k_1^2 \tilde{E}_i \\ -(\bar{E}_i / \tau_E^{sc}) k_1^2 \tilde{E}_i \end{bmatrix}, \tag{26}$$

which reduces (24) to (25). Since $\theta_4^\star > 0$, (23) and (26) guarantee that $\tilde{E}_i$ is driven to zero. Note that (23) can be derived directly from (19) but only in terms of nominal lumped parameters. Lyapunov analysis is required to derive the stabilizing adaptive law (26).

If P_{aux} is calculated to be negative in (23), we set $P_{aux} = 0$ and solve (23) for the desired impurity density, $n_I^\star$, which stabilizes the $\tilde{E}_i = 0$ equilibrium. The adaptive control laws for the particle injection, (38), (39), (40) and (43), are formulated below and guarantee that

$$\hat{n}_I = n_I - n_I^\star, \tag{27}$$

is driven to zero.

As impurities are injected into the plasma, P_{rad} rises and P_{aux} from (23) increases. Eventually, the controller's request for auxiliary power from (23) will become positive. Therefore, $\tilde{E}_i$ will be stabilized at the origin with $P_{aux} \geq 0$. Over time, the desired impurity density, $n_I^\star$, will approach the equilibrium target $\bar{n}_I$. When $n_I^\star = \bar{n}_I$, $\tilde{n}_I = \hat{n}_I$. As stated previously, the fueling adaptive control laws, (38), (39), (40) and (43), guarantee that $\hat{n}_I \to 0$. Therefore, $\tilde{n}_I \to 0$.

Density Control: In order to derive adaptive control laws for the fueling actuators (S_D, S_T, S_I), we take the second Lyapunov function

$$V_S = \frac{k_2^2\tilde{\gamma}^2 + \tilde{n}^2 + \hat{n}_I^2}{2} + \tilde{\theta}_S^T \frac{\Omega^{-1}}{2}\tilde{\theta}_S, \tag{28}$$

where $\tilde{\gamma} \triangleq \gamma - \bar{\gamma}$ is the deviation from the desired tritium fraction, $\tilde{n} \triangleq n - \bar{n}$ is the deviation from the desired plasma density, $\tilde{\theta}_S = [\tilde{\theta}_5 \quad \tilde{\theta}_6 \quad \tilde{\theta}_7 \quad \tilde{\theta}_8 \quad \tilde{\theta}_9 \quad \tilde{\theta}_{10} \quad \tilde{\theta}_{11} \quad \tilde{\theta}_{12}]^T$ is defined in the same way as $\tilde{\theta}_E$, i.e. $\tilde{\theta}_S = \hat{\theta}_S - \theta_S^\star$, Ω is positive definite, and k_2 is a positive constant. The time derivative of (28) is given by

$$\dot{V}_S = k_2^2\tilde{\gamma}\dot{\tilde{\gamma}} + \tilde{n}\dot{\tilde{n}} + \hat{n}_I\dot{\hat{n}}_I + \tilde{\theta}_S^T\Omega^{-1}\dot{\tilde{\theta}}_S. \tag{29}$$

Since $\dot{\theta}_S^\star = 0$, $\dot{\tilde{\theta}}_S = \dot{\hat{\theta}}_S$. The dynamics of the control variables must be determined. The dynamics of (13) is

$$\dot{\gamma} = \dot{\tilde{\gamma}} = \frac{\dot{n}_T n_H - n_T \dot{n}_H}{n_H^2} = \frac{\dot{n}_T}{n_H} - \gamma\frac{\dot{n}_H}{n_H}, \tag{30}$$

where

$$\begin{aligned}\dot{n}_H = \dot{\tilde{n}}_H = \dot{\tilde{n}}_T + \dot{\tilde{n}}_D = &-\theta_7^\star\frac{n_T}{\tau_E^{sc}} - \theta_6^\star\frac{n_D}{\tau_E^{sc}} + S_D \\ &+ S_T - 2S_\alpha + \theta_9^\star\frac{n_T}{\tau_E^{sc}} + \theta_{10}^\star\frac{n_D}{\tau_E^{sc}}.\end{aligned} \tag{31}$$

Therefore, we can recall (18) to write the dynamics of $\tilde{\gamma}$, i.e.

$$\begin{aligned}\dot{\tilde{\gamma}} = \frac{1}{n_H}\Bigg[&- \theta_7^\star\frac{n_T}{\tau_E^{sc}} - S_\alpha + S_T + \theta_{10}^\star\frac{n_D}{\tau_E^{sc}} - \gamma\Bigg(- \theta_7^\star\frac{n_T}{\tau_E^{sc}} \\ &- \theta_6^\star\frac{n_D}{\tau_E^{sc}} - 2S_\alpha + S_D + S_T + \theta_9^\star\frac{n_T}{\tau_E^{sc}} + \theta_{10}^\star\frac{n_D}{\tau_E^{sc}}\Bigg)\Bigg].\end{aligned} \tag{32}$$

Recalling (3) and (4), the dynamics governing $\tilde{n}$ is

$$\dot{\tilde{n}} = \dot{n} = 3\dot{\tilde{n}}_\alpha + 2\dot{\tilde{n}}_T + 2\dot{\tilde{n}}_D + (Z_I+1)\dot{\tilde{n}}_I, \tag{33}$$

$$\begin{aligned}\dot{\tilde{n}} = &- 3\theta_5^\star\frac{n_\alpha}{\tau_E^{sc}} - 2\theta_7^\star\frac{n_T}{\tau_E^{sc}} - 2\theta_6^\star\frac{n_D}{\tau_E^{sc}} - (Z_I+1)\theta_8^\star\frac{n_I}{\tau_E^{sc}} \\ &- S_\alpha + 2S_D + 2S_T + (Z_I+1)S_I + 2\theta_9^\star\frac{n_T}{\tau_E^{sc}} \\ &+ 2\theta_{10}^\star\frac{n_D}{\tau_E^{sc}} + (Z_I+1)\theta_{11}^\star\frac{n}{\tau_E^{sc}} + (Z_I+1)\theta_{12}^\star\dot{n}.\end{aligned} \tag{34}$$

Finally, (27) is used to write

$$\dot{n}_I = \dot{\hat{n}}_I + \dot{n}_I^\star = -\theta_8^\star\frac{n_I}{\tau_E^{sc}} + S_I + \theta_{11}^\star\frac{n}{\tau_E^{sc}} + \theta_{12}^\star\dot{n}, \tag{35}$$

$$\dot{\hat{n}}_I = - \theta_8^\star\frac{n_I}{\tau_E^{sc}} + S_I + \theta_{11}^\star\frac{n}{\tau_E^{sc}} + \theta_{12}^\star\dot{n} - \dot{n}_I^\star. \tag{36}$$

Substituting (32), (34) and (36) into (29) gives

$$\begin{aligned}\dot{V}_S = &\frac{k_2^2\tilde{\gamma}}{n_H}\Bigg[- \theta_7^\star\frac{n_T}{\tau_E^{sc}} - S_\alpha + S_T + \theta_{10}^\star\frac{n_D}{\tau_E^{sc}} - \gamma\Bigg(- \theta_7^\star\frac{n_T}{\tau_E^{sc}} \\ &- \theta_6^\star\frac{n_D}{\tau_E^{sc}} - 2S_\alpha + S_D + S_T + \theta_9^\star\frac{n_T}{\tau_E^{sc}} + \theta_{10}^\star\frac{n_D}{\tau_E^{sc}}\Bigg)\Bigg] \\ &+ \tilde{n}\Bigg[- 3\theta_5^\star\frac{n_\alpha}{\tau_E^{sc}} - 2\theta_7^\star\frac{n_T}{\tau_E^{sc}} - 2\theta_6^\star\frac{n_D}{\tau_E^{sc}} + 2S_D + 2S_T \\ &- S_\alpha - (Z_I+1)\theta_8^\star\frac{n_I}{\tau_E^{sc}} + (Z_I+1)S_I + 2\theta_9^\star\frac{n_T}{\tau_E^{sc}} \\ &+ 2\theta_{10}^\star\frac{n_D}{\tau_E^{sc}} + (Z_I+1)\theta_{11}^\star\frac{n}{\tau_E^{sc}} + (Z_I+1)\theta_{12}^\star\dot{n}\Bigg] \\ &+ \hat{n}_I\Bigg[- \theta_8^\star\frac{n_I}{\tau_E^{sc}} + S_I + \theta_{11}^\star\frac{n}{\tau_E^{sc}} + \theta_{12}^\star\dot{n} - \dot{n}_I^\star\Bigg] \\ &+ \tilde{\theta}_S^T\Omega^{-1}\dot{\tilde{\theta}}_S.\end{aligned} \tag{37}$$

Because of the certainty equivalence principle, we take the control laws

$$\begin{aligned}S_D = &\frac{1}{2}\Bigg[3\hat{\theta}_5\frac{n_\alpha}{\tau_E^{sc}} + 2\hat{\theta}_7\frac{n_T}{\tau_E^{sc}} + 2\hat{\theta}_6\frac{n_D}{\tau_E^{sc}} + S_\alpha - 2S_T \\ &- (Z_I+1)\Bigg(S_I - \hat{\theta}_8\frac{n_I}{\tau_E^{sc}}\Bigg) - 2\hat{\theta}_9\frac{n_T}{\tau_E^{sc}} - 2\hat{\theta}_{10}\frac{n_D}{\tau_E^{sc}} \\ &- (Z_I+1)\hat{\theta}_{11}\frac{n}{\tau_E^{sc}} - (Z_I+1)\hat{\theta}_{12}\dot{n} - K_n\tilde{n}\Bigg],\end{aligned} \tag{38}$$

$$\begin{aligned}S_T = &- K_\gamma\tilde{\gamma} + \hat{\theta}_7\frac{n_T}{\tau_E^{sc}} + S_\alpha - \hat{\theta}_{10}\frac{n_D}{\tau_E^{sc}} \\ &+ \gamma\Bigg(\hat{\theta}_5\frac{3n_\alpha}{2\tau_E^{sc}} - \frac{3}{2}S_\alpha - \frac{(Z_I+1)}{2}\Bigg(S_I - \hat{\theta}_8\frac{n_I}{\tau_E^{sc}}\Bigg) \\ &- \frac{(Z_I+1)}{2}\hat{\theta}_{11}\frac{n}{\tau_E^{sc}} - \frac{(Z_I+1)}{2}\hat{\theta}_{12}\dot{n} - \frac{K_n\tilde{n}}{2}\Bigg),\end{aligned} \tag{39}$$

$$S_I = \hat{\theta}_8\frac{n_I}{\tau_E^{sc}} + \dot{n}_I^\star - \hat{\theta}_{11}\frac{n}{\tau_E^{sc}} - \hat{\theta}_{12}\dot{n} - K_I\hat{n}_I, \tag{40}$$

where K_n, K_γ and K_I are positive constants. Equation (37) is then reduced to

$$\begin{aligned}\dot{V}_S = &- K_\gamma\frac{k_2^2\tilde{\gamma}^2}{n_H} - K_n\tilde{n}^2 - K_I\hat{n}_I^2 + \tilde{\theta}^T\Omega^{-1}\dot{\tilde{\theta}} \\ &+ \Bigg(2\tilde{n} - \frac{k_2^2\tilde{\gamma}}{n_H}\gamma\Bigg)\frac{n_D}{\tau_E^{sc}}\tilde{\theta}_6 + \Bigg(2\tilde{n} - (\gamma-1)\frac{k_2^2\tilde{\gamma}}{n_H}\Bigg)\frac{n_T}{\tau_E^{sc}}\tilde{\theta}_7 \\ &+ \Bigg(\frac{k_2^2\tilde{\gamma}}{n_H}\gamma - 2\tilde{n}\Bigg)\frac{n_T}{\tau_E^{sc}}\tilde{\theta}_9 + (\gamma-1)\frac{k_2^2\tilde{\gamma}}{n_H}\frac{n_D}{\tau_E^{sc}}\tilde{\theta}_{10} \\ &- (\tilde{n}(Z_I+1) + \hat{n}_I)\frac{n}{\tau_E^{sc}}\tilde{\theta}_{11} - (\hat{n}_I + (Z_I+1)\tilde{n})\dot{n}\tilde{\theta}_{12} \\ &+ 3\tilde{n}\frac{n_\alpha}{\tau_E^{sc}}\tilde{\theta}_5 + (\tilde{n}(Z_I+1) + \hat{n}_I)\frac{n_I}{\tau_E^{sc}}\tilde{\theta}_8.\end{aligned} \tag{41}$$

TABLE I: Uncertain Parameters

Parameter	Nominal Value	Initial Estimate
ρ	0.85	1.05
H_H	1	1.1
k_α	7	10
k_D	3.2	3.8
k_T	2.8	3.8
k_I	10	9
f_{ref}	0.5	0.35
f_{eff}	0.3	0.45
R^{eff}	0.9	0.75
γ^{PFC}	0.5	0.52
f_I^{sp}	0.01	0.015

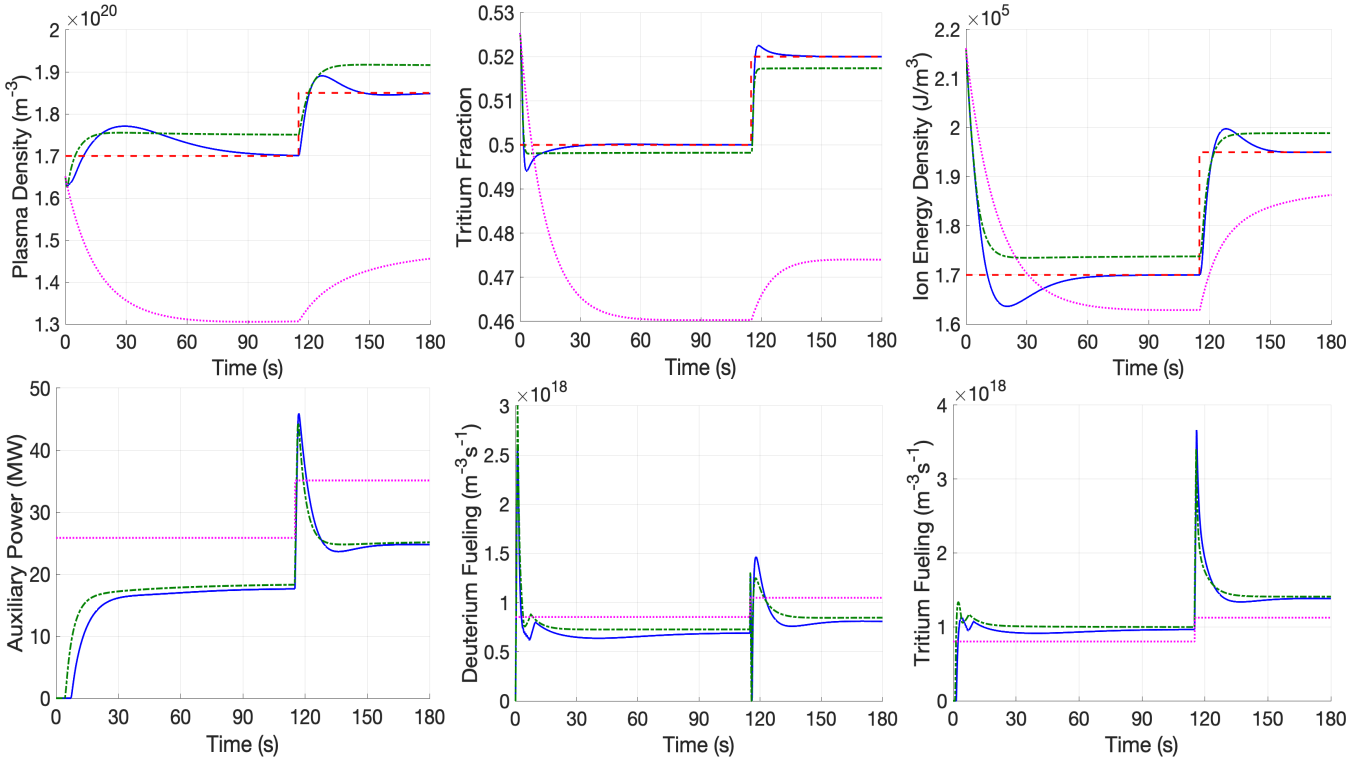

Fig. 1: Time evolutions of the control variables and actuators under open-loop (magenta dotted), closed-loop (green dashed-dotted) and adaptive control (blue solid) are shown. At 115s, the equilibrium point changes. The system successfully tracks the desired equilibrium (red dashed) only if adaptation is on.

With exact knowledge of the lumped nominal parameters ($\hat{\theta}_S = \theta_S^\star \Leftrightarrow \tilde{\theta}_S \equiv 0$),

$$\dot{V}_S = -K_\gamma \frac{k_2^2 \tilde{\gamma}^2}{n_H} - K_n \tilde{n}^2 - K_I \hat{n}_I^2 \leq 0. \tag{42}$$

Generally, the controller will have to rely on estimates of the lumped parameters. Therefore, we take the adaptive law

$$\dot{\hat{\theta}}_S = \dot{\tilde{\theta}}_S = \Omega \begin{bmatrix} -3\tilde{n}\dfrac{n_\alpha}{\tau_E^{sc}} \\ -\left(2\tilde{n} - \dfrac{k_2^2\tilde{\gamma}}{n_H}\gamma\right)\dfrac{n_D}{\tau_E^{sc}} \\ -\left(2\tilde{n} - (\gamma-1)\dfrac{k_2^2\tilde{\gamma}}{n_H}\right)\dfrac{n_T}{\tau_E^{sc}} \\ -(\tilde{n}(Z_I+1)+\hat{n}_I)\dfrac{n_I}{\tau_E^{sc}} \\ -\left(\dfrac{k_2^2\tilde{\gamma}}{n_H}\gamma - 2\tilde{n}\right)\dfrac{n_T}{\tau_E^{sc}} \\ -(\gamma-1)\dfrac{k_2^2\tilde{\gamma}}{n_H}\dfrac{n_D}{\tau_E^{sc}} \\ (\tilde{n}(Z_I+1)+\hat{n}_I)\dfrac{n}{\tau_E^{sc}} \\ (\hat{n}_I + (Z_I+1)\tilde{n})\dot{n} \end{bmatrix}, \tag{43}$$

which reduces (41) to (42). The control laws (38), (39) and (40) and the adaptive law (43) drive γ, n and $\hat{n}_I$ to their desired values.

The two inputs of the energy subsystem ($\tilde{E}_i$) are P_{aux} and n_I, where n_I is an output of the density subsystem ($\tilde{\gamma}$, $\tilde{n}$, $\hat{n}_I$). This describes a cascade system [9]. When $n_I = n_I^\star$ ($\Rightarrow \hat{n}_I \equiv 0$), the origin of the $\tilde{E}_i$ subsystem is asymptotically stable by satisfying (19). During the transient $n_I \neq n_I^\star$, $\tilde{E}_i$ is bounded for a bounded input n_I. The impurity density is bounded due to a maximum impurity pellet injection rate. Moreover, the saturation of particle injection rates (S_D, S_T, S_I) imposes a limit on the radiative losses, maintaining boundedness of the state $\tilde{E}_i$. Therefore, the $\tilde{E}_i$ subsystem is input-to-state stable (ISS) with respect to n_I. The fueling adaptive control laws, (38), (39), (40) and (43), assure asymptotic stability of the origin of the density subsystem. Because of the ISS property of the energy subsystem with respect to input n_I and the asymptotic stability of the equilibrium of the density subsystem, the cascade system is asymptotically stable. Therefore, the adaptive control laws (23), (26), (38), (39), (40), (43) derived from V_E and V_S guarantee stability of the equilibrium at the origin of the overall system ($\tilde{E}_i$, $\tilde{\gamma}$, $\tilde{n}$, $\hat{n}_I$). These adaptive laws do not guarantee however that the estimation errors of the uncertain parameters converge to zero, but this was not the design goal.

To show that $\tilde{n}_\alpha \to 0$ once $\tilde{E}_i, \tilde{\gamma}, \tilde{n}, \hat{n}_I \to 0$, the Lyapunov function $V_\alpha = \tilde{n}_\alpha^2/2$ with derivative $\dot{V}_\alpha = \tilde{n}_\alpha(-\theta_5^\star n_\alpha/\tau_E^{sc} + S_\alpha)$ is considered. When $E_i = \bar{E}_i$, $\gamma = \bar{\gamma}$, $n = \bar{n}$ and $n_I = \bar{n}_I$, the terms $-\theta_5^\star n_\alpha/\tau_E^{sc}$ and S_α decrease with increasing n_α and vice versa. If μ is a positive continuous function, then the sum of these two terms can be replaced with $-\mu\tilde{n}_\alpha$ and $\dot{V}_\alpha = -\tilde{n}_\alpha^2\mu \leq 0$ for $\tilde{E}_i = \tilde{\gamma} = \tilde{n} = \tilde{n}_I = 0$.

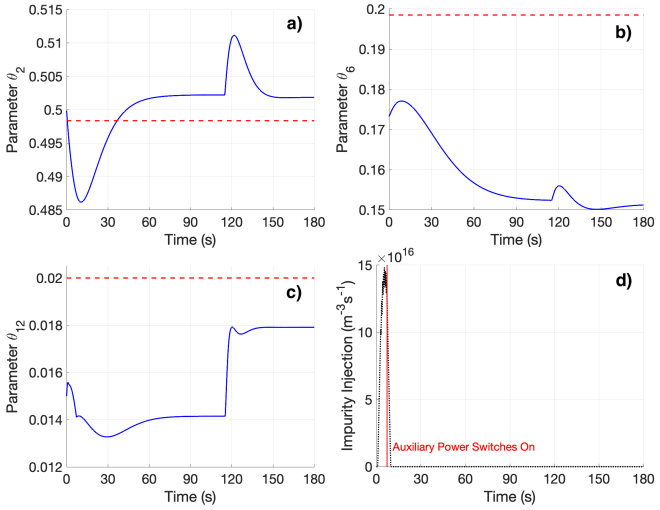

Fig. 2: a, b, c) Adaptive estimation of three lumped parameters $\hat{\theta}_i$ (blue solid) and their nominal values $\theta_i^\star$ (red dashed) are presented. The excluded $\hat{\theta}_i$ behave similarly to the three shown. d) During the simulation with adaptation, impurity injection (black dotted) is utilized while the auxiliary power is saturated at zero. Once the auxiliary power switches on (red solid), the controller stops injecting impurities.

V. SIMULATION STUDY

In this section, we present simulations to assess the performance of the proposed adaptive control scheme. We test for robustness by perturbing the initial estimates of the uncertain parameters. Table I contains the nominal values of the uncertain parameters and their initial estimates used in this study. The initial conditions were $n_\alpha = 2.4 \times 10^{18}\text{m}^{-3}$, $n_D = 3.75 \times 10^{19}\text{m}^{-3}$, $n_T = 4.15 \times 10^{19}\text{m}^{-3}$, $n_I = 0$ and $E_i = 2.16{\times}10^5\text{J/m}^3$. The desired equilibrium initially sent to the controller was that defined by solving the nominal steady-state system (17) with $d/dt = 0$, for $E_i = 1.7 \times 10^5\text{J/m}^3$, $n = 1.7 \times 10^{20}\text{m}^{-3}$ and $\gamma = 0.5$. At 115 seconds, the desired equilibrium was switched to that defined by $E_i = 1.95 \times 10^5\text{J/m}^3$, $n = 1.85 \times 10^{20}\text{m}^{-3}$ and $\gamma = 0.52$. Actuator limits relevant to ITER were used. Assuming 100% purity in the deuterium and tritium fueling lines, the maximum pellet injection rates in ITER would be $S_D = 120\,\text{Pa m}^3\text{/s} \approx 7.60 \times 10^{19}\text{m}^{-3}\text{s}^{-1}$ and $S_T = 111\,\text{Pa m}^3\text{/s} \approx 7.03 \times 10^{19}\text{m}^{-3}\text{s}^{-1}$. The maximum impurity pellet injection rate is $S_I = 10\,\text{Pa m}^3\text{/s} \approx 6.34 \times 10^{18}\text{m}^{-3}\text{s}^{-1}$. ITER is planned to have 73 MW of available auxiliary power [14]. The atomic number of the impurity was taken to be $Z_I = 6$.

We compare the adaptive control simulation to both a closed-loop simulation without adaptation and an open-loop simulation. The constant open-loop values of $\bar{S}_D$, $\bar{S}_T$ and $\bar{P}_{aux}$ were determined by again solving (17) with $d/dt = 0$ for the desired E_i, n and γ, but we used the initial parameter estimates from Table I instead ($\theta_i^\star \to \hat{\theta}_i$). Fig. 1 shows the time evolution of the control variables and actuators during the three simulations. The adaptive controller successfully drives the system to the desired operating points, while the non-adaptive controller fails. When the system is regulated by open-loop actuation, it moves away from the desired equilibrium points. As seen in Fig. 2, the adaptive laws do not guarantee that the estimation errors of the uncertain parameters converge to zero. During the first $\sim$7s of the simulation, a short burst of impurity injection is used to cool the system while the auxiliary heating is turned off (Fig. 2).

VI. CONCLUSIONS AND FUTURE WORK

We have proposed a Lyapunov-based nonlinear controller that uses auxiliary heating and particle injection to force a burning plasma to a desired equilibrium despite numerous model uncertainties. The uncertainty was broad in scope, involving the plasma confinement, wall recycling, and the electron energy. The presented simulation study shows the necessity of a control scheme that can handle large perturbations in initial conditions and parameter estimates. While the adaptive laws cannot be used for parameter identification, they successfully stabilize the system's equilibrium. In our model, we made the simplifying assumption that the electron and ion energies are directly proportional. Future work may involve developing control schemes for a more complex two-temperature 0-D model that considers separate time-dependent energy balance equations for the ions and electrons. Such a controller would assume the the electrons and ions can be heated independently with different auxiliary power actuators (i.e. ICRF and ECRH).

REFERENCES

[1] J. Wesson, *Tokamaks*, 3rd ed. Oxford: Clarendon Press, 2004.

[2] S. K. Combs, L. R. Baylor and others, "Overview of recent developments in pellet injection for ITER," Fusion Engineering and Design, vol. 87, pp. 634640, 2012.

[3] E. Schuster, M. Krstic, and G. Tynan, "Burn control in fusion reactors via nonlinear stabilization techniques," *Fusion Science and Technology*, vol. 43, no. 1, pp. 1837, 2002.

[4] S. W. Haney, L. J. Perkins, J. Mandrekas and W. M. Stacey, Jr., "Active control of burn conditions for the international thermonuclear experimental reactor", Fusion Technology, vol. 18, no. 4, pp. 606-17, 1990.

[5] J. Mandrekas and W. M. Stacey Jr., "Evaluation of different burn control methods for the International Thermonuclear Experimental Reactor," *Proceedings of the 13th IEEE Symposium on Fusion Engineering*, vol. 1, pp. 404407, 1989.

[6] J. Ehrenberg, "Wall effects on particle recycling in tokamaks," in *Physical processes of the interaction of fusion plasmas with solids*, p. 35, Academic Press, 1996.

[7] M. D. Boyer and E. Schuster, "Adaptive nonlinear burn control in tokamak fusion reactors," *Proceedings of the American Control Conference*, pp. 5043-5048, 2012.

[8] M. D. Boyer and E. Schuster, "Nonlinear Burn Control in Tokamak Fusion Reactors via Output Feedback," *IFAC Proceedings Volumes*, vol. 47, no. 3, 2014

[9] H. Khalil, *Nonlinear Systems*, 3rd ed. New Jersey: Prentice Hall, 2001.

[10] L. Hively, "Special topic convenient computational forms for maxwellian reactivities," *Nucl. Fusion*, vol. 17, no. 4, pp. 873, 1977.

[11] W. M. Stacey, "Fusion: An introduction to the physics and technology of magnetic confinement fusion," *Wiley-VHC, Weinheim, 2nd edition,* 2010.

[12] "Summary of the ITER final design report," *Technical Report, International Atomic Energy Agency*, 2001.

[13] Krstić, Kanellakopoulos and Kokotović, "Nonlinear and Adaptive Control Design," *Wiley*, 1995.

[14] J.A. Snipes, D. Beltran and others, "Actuator and diagnostic requirements of the ITER Plasma Control System," *Fusion Engineering and Design*, vol. 87, no. 12, pp. 1900-1906, 2012.